Article

The Use of H-SAF Soil Moisture Products for Operational Hydrology: Flood Modelling over Italy

Christian Massari [1],*, Luca Brocca [1], Luca Ciabatta [1], Tommaso Moramarco [1], Simone Gabellani [2], Clement Albergel [3], Patricia De Rosnay [3], Silvia Puca [4] and Wolfgang Wagner [5]

[1] Research Institute for Geo-Hydrological Protection, National Research Council CNR, Via di Madonna Alta 126, 06128 Perugia, Italy; E-Mails: luca.brocca@irpi.cnr.it (L.B.); luca.ciabatta@irpi.cnr.it (L.C.); tommaso.moramarco@irpi.cnr.it (T.M.)

[2] International Centre on Environmental Monitoring (CIMA) Research Foundation, Via A. Magliotto, 2-17100 Savona, Italy; E-Mail: simone.gabellani@cimafoundation.org

[3] European Centre for Medium-Range Weather Forecasts (ECMWF), Shinfield Park, RG2 9AX Reading, UK; E-Mails: clement.albergel@ecmwf.int (C.A.); Patricia.Rosnay@ecmwf.int (P.D.R.)

[4] Italian Civil Protection Department, Via Vitorchiano 2, 00189 Rome, Italy; E-Mail: Silvia.Puca@protezionecivile.it

[5] Department of Geodesy and Geoinformation, Vienna University of Technology, 1040 Vienna, Austria; E-Mail: wolfgang.wagner@geo.tuwien.ac.at

* Author to whom correspondence should be addressed; E-Mail: christian.massari@irpi.cnr.it; Tel.: +39-075-501-4417.

Academic Editor: Okke Batelaan

Abstract: The ever-increasing availability of new remote sensing and land surface model datasets opens new opportunities for hydrologists to improve flood forecasting systems. The current study investigates the performance of two operational soil moisture (SM) products provided by the "EUMETSATSatellite Application Facility in Support of Operational Hydrology and Water Management" (H-SAF, http://hsaf.meteoam.it/) within a recently-developed hydrological model called the "simplified continuous rainfall-runoff model" (SCRRM) and the possibility of using such a model at an operational level. The model uses SM datasets derived from external sources (*i.e.*, remote sensing and land surface models) as input for calculating the initial wetness conditions of the catchment prior to

the flood event. Hydro-meteorological data from 35 Italian catchments ranging from 800 to 7400 km^2 were used for the analysis for a total of 593 flood events. The results show that H-SAF operational products used within SCRRM satisfactorily reproduce the selected flood events, providing a median Nash–Sutcliffe efficiency index equal to 0.64 (SM-OBS-1) and 0.60 (SM-DAS-2), respectively. Given the results obtained along with the parsimony, the simplicity and independence of the model from continuously-recorded rainfall and evapotranspiration data, the study suggests that: (i) SM-OBS-1 and SM-DAS-2 contain useful information for flood modelling, which can be exploited in flood forecasting; and (ii) SCRRM is expected to be beneficial as a component of real-time flood forecasting systems in regions characterized by low data availability, where a continuous modelling approach can be problematic.

Keywords: soil moisture; floods; remote sensing; hydrological modelling

---

1. Introduction

Flooding has become one of the events producing the most fatalities annually [1]. Whereas much progress has been made in meteo-forecasts and warnings and also in public preparedness, a comparable system for "quantitatively" predicting floods has experienced less progress, especially in floods occurring in medium–small catchment sizes (100–1000 km^2), as demonstrated by recent events occurring in Italy (*i.e.*, Liguria, Tuscany and Sicily at the end of 2011, Umbria in 2012 and Sardinia in 2014).

Indeed, the anticipation of the magnitude of an event is crucial for performing the correct actions within civil protection activities, but this is not a simple task. First, the amount of precipitation that transforms an otherwise ordinary rainfall event into an extraordinary one is led by complex interactions between meteorology and hydrology, such as, among other important factors, the soil moisture (SM) conditions prior to the flood event [2–5]. Second, predicting a flood event is not only a matter of being able to correctly describe such factors, but it is strongly related to the capability of the early warning system in terms of the data and tools upon which it can rely. That is: (i) an appropriate rainfall-runoff (RR) hydrological model able to infer, with a certain degree of accuracy, the discharge hydrograph; and (ii) a dense network of sensors able to provide good quality observations in near real time.

These two requirements are not independent of each other. Indeed, the choice of the most appropriate RR model (e.g., continuous *versus* event-based models) often stems from the availability of certain types of data (e.g., evapotranspiration or temperature data) and from the number of sensors available in the catchment, which leads the hydrologist to the choice of a continuous, event-based, distributed or lumped hydrological model.

Generally, continuous models try to describe the different hydrological processes able to generate runoff, but require long-term and uninterrupted time series of rainfall and evapotranspiration data. This could be a strong limitation in poorly-gauged areas, mainly if hourly observations are needed [6]. On the other hand, event-based RR models are very appealing and frequently employed within operational flood forecasting systems [3], because of their simplicity, the need for reduced

parametrization and data records (*i.e.*, only rainfall recorded during the event is needed) and last, but not least, the much lower computational demand. However, a major limitation of event-based models lies in the definition of the initial SM conditions of the catchment, which may strongly vary from one storm event to another [3,5,7], especially in regions characterized by strong seasonality, such as Mediterranean countries [8].

In the last few decades, many studies [4,5,9–13] have mentioned the high importance of SM, because of its ability to determine the partitioning of rainfall into runoff and infiltration [14]. In particular, the authors have demonstrated that when SM is characterized by high variability throughout the year (e.g., in Mediterranean regions), it represents, more than others quantities, a good proxy of the antecedent wetness conditions of the catchment, thus allowing better prediction of the runoff response to the rainfall input.

At the same time, the ever-increasing availability of SM measurements from *in situ* stations (International Soil Moisture Network (ISMN) [15]), satellite sensors (e.g., the Advanced Scatterometer (ASCAT), [16], the Advanced Microwave Scanning Radiometer for Earth observation (AMSR-E) and its successor, AMSR-2 [17], and the Soil Moisture and Ocean Salinity Mission (SMOS) [18]) and land surface models [19], at increasing temporal and spatial resolutions [20], has opened new possibilities for integrating such measurements into hydrological models, even at an operational level. By way of example, the "EUMETSAT Satellite Application Facility in Support of Operational Hydrology and Water Management" (H-SAF, http://hsaf.meteoam.it/), established by the EUMETSAT Council in 2005, generates and archives high-quality rainfall, soil moisture and snow products for operational hydrological applications, starting from the acquisition and processing of data from Earth observation satellites in geostationary and polar orbits operated both by EUMETSAT and other satellite organizations.

Such an overabundance of products has highly increased the number of studies concerning the assimilation of SM into hydrological models (the reader is referred to [21] for a complete review of these studies). Although many of them show very contrasting results in terms of how the assimilation of SM can improve the accuracy in flood forecasting, all seem to agree that such observations have a high potential to reduce uncertainty in flood prediction. The problem is more related to the preprocessing steps prior to the inclusion of the observations into the hydrological model [22] and in the correct use of the assimilation technique [23], rather than in the value that the observations themselves can bring to flood forecasting. At an operational level, especially in small–medium catchments, the problem is even more exacerbated, due to: (i) the high level of expertise required for implementing and setting up an appropriate assimilation scheme with the risk of not even exploiting these new source of data; and (ii) the lack of uninterrupted and good quality rainfall and evapotranspiration data for running continuous hydrological models, which are needed for current data assimilation approaches.

Recently, [24] proposed a "simplified continuous rainfall runoff model" (SCRRM) that, instead of modelling SM from continuous precipitation and evapotranspiration data, like in classical continuous RR models [12,25–27], directly uses SM recorded from external sources (e.g., ground observations, satellite sensors and land surface models) to set the initial conditions of an event-based model. SCRRM explicitly embeds the relationship existing between SM and the model's initial conditions [2–5] into an event-based RR model to simulate discharge hydrographs. The model was successfully applied in a small catchment of the Attica Region in Greece using different globally-available SM and yielding

performances similar to a continuous model [24]. The main advantages of this approach are that SCRRM: (i) does not require continuously-recorded datasets; hence, it can be used also in poorly-gauged areas; (ii) is simple and parsimonious, which is an advantage for users with low hydrological expertise; (iii) requires low computational demand to be run, which makes it appropriate for early warning system applications operating in near real time; and (iv) can be used to "hydro-validate" satellite soil moisture observations. For these reasons, the model is very attractive for civil protection activities, especially in areas where a flood forecasting system is totally absent, and for testing the information content related to the satellite SM dataset.

Based on that, the objectives of this study are two-fold. The first goal is to investigate the performance of two of the satellite SM products of the H-SAF project (*i.e.*, SM-OBS-1 and SM-DAS-2) in order to highlight the information content that they retain in flood modelling. The second goal is to test the performance of SCRRM against the "Modello Idrologico Semi-Distribuito in continuo" (MISDc, [12]) over the Italian territory in order to gain some understanding regarding under what conditions the information derived from the external source of SM can be used for flood forecasting at an operational level.

A total of 593 flood events are used, extracted from a dataset of rainfall and discharges recorded from 2010 to 2013 of 35 Italian catchments, representing a range of sizes, micro-climates, precipitation, streamflows and SM conditions. Through the analysis of such a large number of catchments, some understanding may be gained regarding under what conditions the information derived from the external source of SM can be used for flood forecasting at an operational level.

The paper is organized as follows: In Section 2, we describe the hydrological models used in this study and the characteristics of the selected catchments. In Section 3, we provide a comprehensive analysis of SCRRM performances running with SM-OBS-1 and SM-DAS-2, comparing it against the "Modello Idrologico Semi-Distribuito in continuo" (MISDc, [12]) in terms of reproducing the discharge hydrograph, the peak discharge and the total runoff volume. Finally, in Section 4, we provide the conclusions.

2. Data and Methods

2.1. Catchment Selection and Hydro-Meteorological Data

An available dataset (2010–2013) of 35 Italian catchments having hourly streamflow, precipitation and temperature observations provided by the Italian Civil Protection Department (DPC) was used in the present analysis (see Table 1 for more details). The catchments range in size from 800 to 7400 km^2 (mean size 2507 km^2). Most catchments are located in the northern part of Italy (see Figure 1). This region is characterized by a temperate Mediterranean climate with a wet winter and moderate summer rainfall, whereas the south part of Italy has a drier climate with semi-arid summers and temperate winters. The number of catchments is the result of an appropriate selection for excluding catchments with streamflow subject to regulation or diversion and characterized by a number of events less than three. The mean areal rainfall for each catchment was calculated by the GRISO model [28]. GRISO is an improved Kriging-based technique that preserves the values observed at the rain gauge location, allowing for a dynamical definition of the covariance structure associated with each rain gauge by

the interpolation procedure. Each correlation structure may depend both on the rain gauge location and on the accumulation time considered. Rainfall events were extracted by selecting those with a continuous rainfall characterized by a total cumulated precipitation larger than 10 mm and no rainfall in the preceding day for a total of 593 flood events. Direct runoff was evaluated as in [29] by using an appropriate base flow separation technique. Mean temperature data for the catchments were obtained by averaging the temperature recorded by the thermometers inside the catchment boundaries.

Figure 1. Approximative catchment position.

Table 1. Characteristics of the selected catchments.

#	Code	Catchment	Longitude E	Latitude N	Area (km^2)	No. Events	Mean Annual Rainfall (mm)	Temperature (°C)
1	AN-LN	Aniene at Lunghezza	12.66	41.93	984.6	5	1525.9	13
2	BA-MG	Bacchiglione at Montegalda	11.67	45.44	1321.3	18	2759.5	10.2
3	BO-AL	Bormida at Alessandria	8.65	44.91	2355.8	18	1157.6	11.6
4	BR-BZ	Brenta at Berzizza	11.73	45.78	1506.3	8	2255.1	7
5	DO-AV	Dorabaltea at Verolengo	8.04	45.19	3640.8	11	1089.7	4.4
6	GO-ST	Gorzone at Stanghella	11.76	45.15	1205.8	5	1901.5	13.6
7	MA-CA	Magra at Calamazza	9.95	44.2	857.8	26	2807.7	11.3
8	MA-RC	Maira at Raconigi	7.67	44.77	967.8	8	998.2	7.9
9	ME-ME	Metauro at Metauro	12.97	43.76	1206.4	13	1617.9	12.6
10	PI-PP	Piave at Pontedipiave	12.45	45.71	3902.7	11	2693.3	6.8
11	PO-CA	Po at Carignano	7.69	44.91	3569.5	9	993.6	8.7
12	PO-MC	Po at Moncalieri	7.68	45	4624.1	9	978.9	9.7
13	PO-MR	Po at Torino Murazzi	7.7	45.06	4899.9	9	986.3	9.7
14	SA-PA	Sangro at Paglieta	14.51	42.21	1522.8	4	1203.6	10.1
15	SE-PS	Sele at Persano Sele	15.03	40.54	2057.9	18	1556.9	12.5
16	ST-LA	Stura di Lanzo at Torino	7.71	45.11	799.9	26	1318.9	7.3
17	ST-MF	Stura di Demonte at Fossano	7.72	44.52	1129.7	8	1300.7	6.3
18	TA-AL	Tanaro at Alba	8.03	44.71	3070.3	20	1170.1	8.8
19	TA-FA	Tanaro at Farigliano	7.9	44.52	1364.5	19	1190.2	9.3
20	TA-MA	Tanaro at Masio	8.41	44.87	4157.4	15	1085.9	9.8
21	TA-MC	Tanaro at Montecastello	8.68	44.95	7400	14	1072.5	10.7
22	TA-SM	Tanaro at Asti San Martino	8.21	44.88	3229.7	14	1154.6	9
23	TE-MM	Tevere at Montemolino	12.39	42.79	4815.4	26	1341.7	12.8
24	TE-PA	Tevere at Pierantonio	12.38	43.26	1694.3	12	1397.7	12.2
25	TE-PF	Tevere at Pontefelcino	12.43	43.13	1879	28	1395.8	12.3
26	TE-PN	Tevere at Pontenuovo	12.43	43.01	3695.3	22	1379.8	12.5
27	TE-SL	Tevere at Santa Lucia	12.24	43.42	837.9	29	1456.9	11.8
28	TO-BE	Topino at Bettona	12.54	43.02	1054.9	24	1333.5	12.6
29	TO-CA	Toce at Candoglia	8.42	45.97	1264	17	1687.9	5.6
30	TR-RG	Trebbia at Rivergaro	9.58	44.9	839.5	27	1735.3	10
31	VO-AM	Volturno at Amorosi	14.45	41.2	1766.8	32	1574.4	13
32	VO-BE	Volturno at Benevento	14.77	41.13	1776.3	34	1173	13.3
33	VO-CA	Volturno at Cancello Arnone	14.02	41.07	4877.9	9	1430.4	13.4
34	VO-GZ	Volturno at Grazzanise	14.11	41.09	4871.1	16	1429.8	13.4
35	VO-SP	Volturno at Solopaca	14.57	41.21	2578.8	29	1307.2	13.3

2.2. Satellite and Modelled Soil Moisture Data

In this study, two different SM products, distributed by the H-SAF project, were used covering the period 2010–2013. The products are SM-OBS-1 (large-scale surface soil moisture by radar scatterometer) and SM-DAS-2 (scatterometer data assimilation in the European Centre for Medium-Range Weather Forecasts, ECMWF, Land Data Assimilation System). Given the different catchment extensions and spatial resolution of the two products, only data falling inside the catchment boundaries were selected (when present). When no pixel was contained inside the boundaries, the closest point to the centroid of the catchment was selected. Pixels near the sea or in very high mountain areas were not considered. Table 2 summarizes the main characteristics of the selected SM indicators, which are described in detail next.

Table 2. The main characteristics of the soil moisture products used in in this study. SM, soil moisture; ASCAT, Advanced Scatterometer.

Product	Code	Spatial Resolution (km)	Temporal Resolution (days)	Depth (cm)	Source
SM-OBS-1	H07	25	$\simeq 1$	0–2	ASCAT
SM-DAS-2	H14	25	1	0–289	Assimilation of SM-OBS-1

2.2.1. SM-OBS-1

Product SM-OBS-1 is based on the radar scatterometer ASCAT onboard the MetOpsatellites. The instrument scans the scene in a push-broom mode by six side-looking antennas, three left-handed and three right-handed. ASCAT measures radar backscatter at the C-band (5.255 GHz) in VV polarization. The basic instrument sampling distance is 12.5 km. The primary ASCAT observation, sea-surface wind, is processed at 50-km resolution. For SM, processing is performed at 50-km (operational) and 25-km (research) resolution. Global coverage over Europe is achieved in ∼1.5 days, while in Italy, measurements are available about once a day. The surface SM product (equivalent to a depth of 0–2 cm of soil) is calculated from the backscatter measurements through a time series-based change detection approach previously used for the ERS-1/2 by [30]. The SM is derived by selecting the historical lowest and highest backscatter measurement to which a 0% (dry) and a 100% (wet) reference is assigned, respectively.

SM-OBS-1 provides knowledge of SM for a very thin surface layer (about 0–2 cm); however, in RR transformation processes, this information may not be sufficient, since the root-zone SM has been shown to be much more important in determining the catchment response to a given storm event [31]. To obtain the root-zone SM product (SWI, Soil Water Index) from the satellite-based surface observations, the recursive formulation [32] of the exponential filter of [30] was adopted:

$$SWI(t_n) = SWI(t_{n-1}) + K_n\left[ms(t_n) - SWI(t_n - 1)\right] \tag{1}$$

where $ms(t_n)$ is the surface SM observed by the satellite sensor SM-OBS-1, SWI_{t_n} is the Soil Wetness Index representing the profile averaged saturation degree and time t_n is the acquisition time of $ms(t_n)$. The gain K_n at time t_n is given by (in a recursive form):

$$K_n = \frac{K_{n-1}}{K_{n-1} + e^{-\left(\frac{t_n - t_{n-1}}{T}\right)}} \tag{2}$$

where T is the characteristic time length expressed in days and represents the time scale of SM variation to obtain the SWI. For the initialization of this filter, K_1 and SWI_1 were set to 1 and $ms(t_1)$, respectively.

2.2.2. SM-DAS-2

SM-DAS-2 is the first global product of consistent surface and root zone SM that is available in near real time for the numerical weather prediction and climate and hydrological communities. It is based on ASCAT surface SM data assimilation in the ECMWF Land Data Assimilation System. Overall, SM-DAS-2 relies on an advanced land data assimilation system, which is based on an extended Kalman filter

(EKF, [33]) able to ingest information contained in observations close to the surface (2-m temperature and relative humidity synoptic report), as well as new types of data, such as remotely-sensed surface SM. Within the EKF, the surface observation from ASCAT is propagated towards the root region down to 289 cm below the surface, providing estimates for 4 layers (thicknesses of 7, 21, 72 and 189 cm). The ECMWF model generates SM profile information according to the Hydrology Tiled ECMWF Scheme for Surface Exchanges over Land (HTESSEL, [19]). SM-DAS-2 is available at a 24-hour time step with a spatial resolution of 25 km, with a global daily coverage at 00:00 UTC. SM-DAS-2 is run continuously in order to ensure the time series consistency of the product (and also to provide values when there is no satellite data, from the model propagation). SM-DAS-2 SM has been validated against *in situ* SM from many locations in Africa, Australia and Europe, providing satisfactory results [34]. It has to be noted that SM-DAS-2 data prior to 2012 are experimental data (*i.e.*, the full 2010–2013 dataset might not be completely consistent), so it is highly expected that it can provide better performances from 2012 onwards.

In this study, the information of the SM for any soil depth between 0 and 289 cm, $\theta_{SM-DAS2}$, was obtained by the weighed mean of the SM provided by the related layer, according to:

$$
\begin{aligned}
\theta_{SM-DAS2} &= \theta_1 & &: z \leq 7 \text{cm} \\
\theta_{SM-DAS2} &= \frac{(\theta_1 7 + \theta_2(z-7))}{z} & &: 7 < z \leq 28 \text{cm} \\
\theta_{SM-DAS2} &= \frac{(\theta_1 7 + \theta_2 21 + \theta_3(z-28))}{z} & &: 28 < z \leq 100 \text{cm} \qquad (3) \\
\theta_{SM-DAS2} &= \frac{(\theta_1 7 + \theta_2 21 + \theta_2 72 + \theta_3(z-100))}{z} & &: 100 < z \leq 289 \text{cm}
\end{aligned}
$$

where $\theta_1, \theta_2, \theta_3, \theta_4$ are the SM for each of the four layers of the SM-DAS-2 product and z is the parameter representing the depth.

2.3. Hydrological Models

In the following, we present a description of all of the hydrological models used for this study. A continuous model (MISDc, "Modello Idrologico Semiditribuito in Continuo", [12]) is used as a benchmark for evaluating the reliability of the SCRRM model presented in Section 2.3.2 running with the two SM products of the H-SAF project described in Section 2.2.

2.3.1. Continuous Model: MISDc

MISDc [12] is a continuous rainfall runoff model successfully applied to the Tiber River for flood prediction and operational purposes. The lumped version of the MISDc model used in this study couples a soil water balance model (SWB, [2]) to simulate the SM temporal pattern and a routing module [35] for transferring the rainfall excess to the outlet section of the catchment. The two models are linked through an experimentally-derived linear relationship between the potential maximum soil moisture retention S of the Soil Conservation Service-Curve Number (SCS-CN, [36]) and the relative SM at the beginning of the event.

The SWB model is a simple water balance model representing the main processes needed for SM simulation: infiltration, percolation and evapotranspiration. The processes are represented for infiltration through the Green–Ampt equation for drainage by a gravity-driven non-linear relationship and for actual evapotranspiration by a linear relationship with the potential evapotranspiration, calculated through a modified Blaney and Criddle method. The reader is referred to [2] and [12] for a detailed description of the model. The SM simulated by the SWB is used to calculate the parameter S method by means of an experimentally-derived relationship between S and SM [10]:

$$S = a(1 - \theta_e) \tag{4}$$

where θ is the modelled relative SM at the beginning of the event and a is a parameter to be estimated. Once the S parameter is estimated, the routing to the outlet of the catchment is obtained from the convolution of the rainfall excess and the geomorphological instantaneous unit hydrograph (GIUH), such as proposed by [37]. In the model, the lag time is evaluated through the relationship proposed by [29]:

$$L = \eta 1.19 A^{0.33} \tag{5}$$

with L being the lag time in hours, A the area of the catchment (km^2), and η the parameter to be calibrated [38].

MISDc requires as input data the rainfall and air temperature. The model outputs are both the direct runoff in correspondence to selected flood events and the catchment average relative SM.
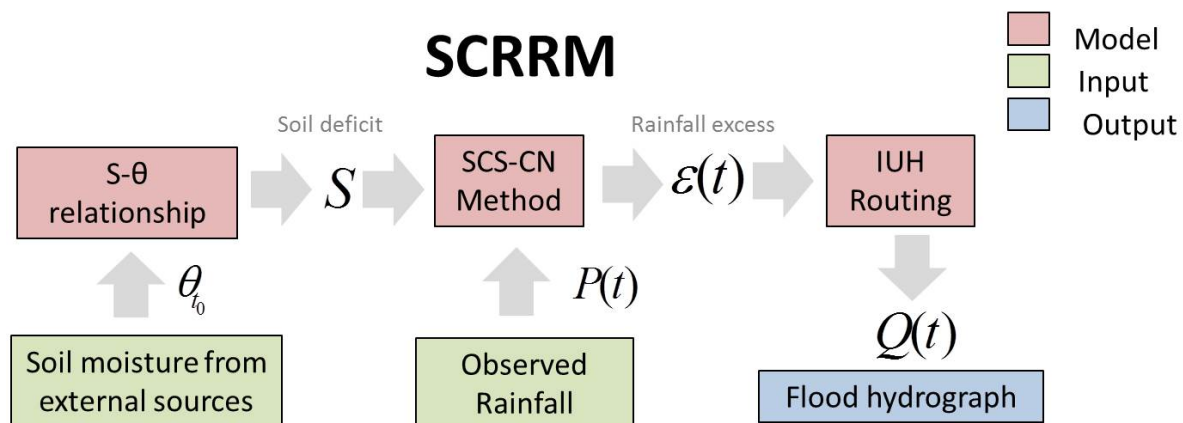

Figure 2. Structure of the simplified continuous rainfall-runoff model (SCRRM).

2.3.2. SCRRM

Unlike MISDc, where the SM at the beginning of the event is simulated by the SWB model, in SCRRM (Figure 2), it is provided by an external indicator, *i.e.*, from satellite SM observations or model-based reanalysis products. SCRRM reflects the structure of MISDc, but has some significant differences. Indeed, the temporal evolution of the soil wetness conditions of the catchment is not modelled from rainfall and temperature data, as in MISDc, but it is integrated directly into the model from SM observations (*i.e.*, SWB is replaced in SCRRM by SM observations immediately before the rainfall event) considering the SM products as proxies for the assessment of the wetness state of the

catchment. The model can be also seen as the result of an assimilation technique in which the SM observations from the external source are assumed to be error free (*i.e.*, a direct insertion technique).

Like in MISDc, the model exploits the observed linear behaviour between the wetness state of the soil and the parameter S of the SCS method by Equation (4). Once S is known, the rainfall excess is calculated by:

$$\epsilon = \frac{(P - F_a)^2}{P - F_a + S} \text{ if } \epsilon \geq F_a \tag{6}$$

where F_a is the initial abstraction, ϵ is the rainfall excess and P is the rainfall depth. As in the SCS method, the quantity F_a is considered linearly dependent on Sby:

$$F_a = \lambda S \tag{7}$$

and then is transferred to the outlet section with the same routing module used by MISDc. In Equation (7), λ is the initial abstraction coefficient.

In synthesis, SCRRM uses the SM and the event rainfall data as the sole inputs to simulate hourly flood hydrographs. Since the SM is provided by an external indicator, Equation (4) becomes a model relation embedded in the model structure. The calibration of the model involves the following three parameters: the coefficient of initial abstractions λ, the parameter a of the $S - \theta$ relationship and the parameter η of Equation (5).

As remarked in Section 2.2, the soil layer depth that controls the RR transformation is usually larger than a few centimetres. As a result, the application of SCRRM with the H-SAF products is taken into account by including the soil depth as an additional parameter of SCRRM. For SM-OBS-1, such a parameter is controlled by the characteristic time length T of the exponential filter described in Section 2.2.1, while for SM-DAS-2, the parameter z of Equation (3) was considered, which can vary from 0 to 289 cm (see Section 2.2.2). For this study, a lumped model was employed, even though the same concept can be easily applied to spatially-distributed models.

2.3.3. Performance Indexes

The performances of SCRRM and MISDc were evaluated by considering different indexes. The first one, commonly used for assessing the agreement between simulated and observed hydrographs, is the Nash–Sutcliffe efficiency coefficient, NS [39]:

$$NS = 1 - \frac{\sum\limits_{t=1}^{T_{ev}} (Q_{obs} - Q_{sim})^2}{\sum\limits_{t=1}^{T_{ev}} (Q_{obs} - \bar{Q}_{obs})^2} \tag{8}$$

where Q_{obs} and Q_{sim} are the observed and simulated discharges at time t, respectively, $\bar{Q}_{obs}$ is the mean value of the observed discharge during the event and T_{ev} is the event duration. NS was calculated for each of the selected events for every catchment considered in the analysis. In particular, the mean NS

calculated over the selected events for each catchment was used as an objective function for calibrating the parameters of the models:

$$\overline{NS} = \frac{\sum\limits_{j=1}^{N_{ev}} NS_j}{N_{ev}} \tag{9}$$

where N_{ev} is the number of events considered, whereas index jvaries between 1 and the number of selected events for each catchment. For model calibration, a standard gradient-based automatic optimisation method (the "fmincon" function in MATLAB ®, [40]) was used. In addition, to evaluate the performance of the model in reproducing flood events, the percentage error on peak discharge:

$$E_{Q_p} = \frac{\max(Q_{obs}) - \max(Q_{sim})}{\max(Q_{obs})} \tag{10}$$

and the percentage error on direct runoff volume:

$$E_V = \frac{\sum\limits_{t}^{T_{ev}} Q_{obs} - \sum\limits_{t}^{T_{ev}} Q_{sim}}{\sum\limits_{t}^{T_{ev}} Q_{obs}} \tag{11}$$

were both evaluated for each single event and as the mean of all of the selected events for every catchment considered in this study.

3. Results and Discussion

In the following, we show the performances obtained by SCRRM using SM-OBS-1 and SM-DAS-2 compared with the results obtained by MISDc. Both MISDc and SCRRM were calibrated using Equation (9) as the objective function and tuning the four parameters of SCRRM and the seven parameters of MISDc. The calibration was carried out separately for each catchment yielding $\overline{NS}$ equal to 0.61, 0.58 and 0.66 for SM-OBS-1, SM-DAS-2 and MISDc, respectively.

In Figure 3(a) and 3(b), the histograms of z and T (*i.e.*, the parameters representing the influence of the soil depth in the RR transformation) show higher frequencies around 1–90 days for T and two main clusters for z: one below 20 cm and the other above 105 cm. The median T and z are about 48 days and 1 m, respectively, which are quite acceptable values in Italy (e.g., [31]). Values of T above 100 days are obtained for catchments PI-PP (Piave at Pontedipiave), AN-LN (Aniene at Lunghezza), BR-BZ (Brenta at Berzizza) and DO-AV (Dorabaltea at Verolengo). These values could be due to several reasons: (i) those related to the influence of a deeper soil layer in the RR transformation (catchments PI-PP and DO-AV have both $T = 300$ days and $z = 80$ cm and 130 cm, which are quite consistent values); (ii) and those related to the accuracy of the observations (e.g., observed discharge datasets), which may affect the consistency of the calibration procedure. Finally, another important reason could be the accuracy of the satellite observations, which results in contrasting T values if compared with z ($z = 6$ cm and $T = 256$ days for catchment BR-BZ).
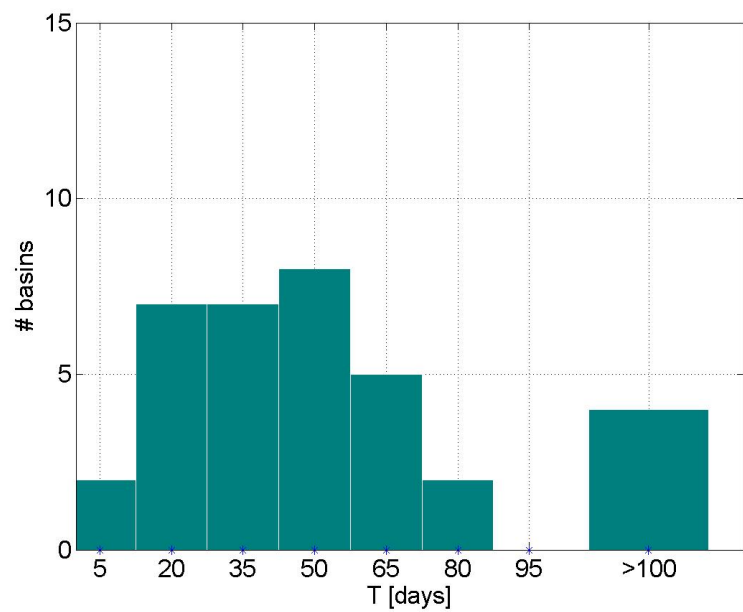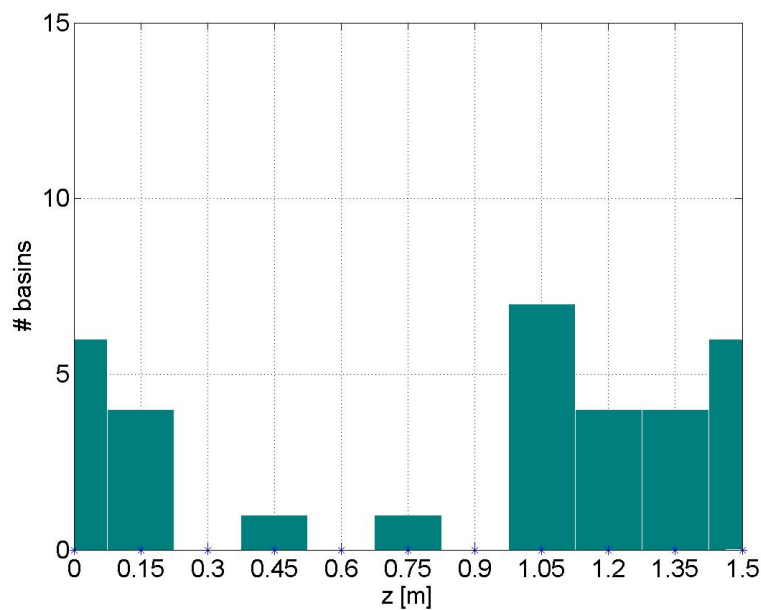
(a) Characteristic time length T

(b) Soil depth z

Figure 3. Histogram of the parameters of SCRRM representing the soil depth involved in the rainfall-runoff transformation. T = characteristic time length used in SCRRM with SM-OBS-1 (**a**); z = soil depth used in SCRRM with SM-DAS-2 (**b**).

Figure 4(a) shows the median NS_{50} obtained by SM-OBS-1, SM-DAS-2 and MISDc for the selected catchments. As can be seen, there is a general agreement between the three configurations, with MISDc being generally better than SM-OBS-1 and SM-DAS-2. The results for E_{Qp50} and E_{V50} in Figure 4(b) and 4(c) reflect those for NS, with the line representing MISDc generally lower than the lines of SM-OBS-1 and SM-DAS-2. The reasons for this could be attributed to: (i) the better description of

the water balance that MISDc can provide with respect to the SCRRM (indeed, MISDc uses the water balance model to "adjust" the initial condition prior to the RR event); (ii) the underlying errors present in the SM estimates and in the coarser resolution of the H-SAF SM products compared to the processes happening at the catchment scale; and (iii) the larger number of parameters of MISDc with respect to SCRRM. It is worth noting that the sensitivity of the selected catchments to the initial conditions was tested by running the SCRRM model with a constant value of soil moisture (*i.e.*, equal to the mean of the soil moisture values associated with the events selected for each catchment). For both products, a sensible reduction of 15% was found for mean NS and an increase of 6% for both E_{Qp} and E_V.
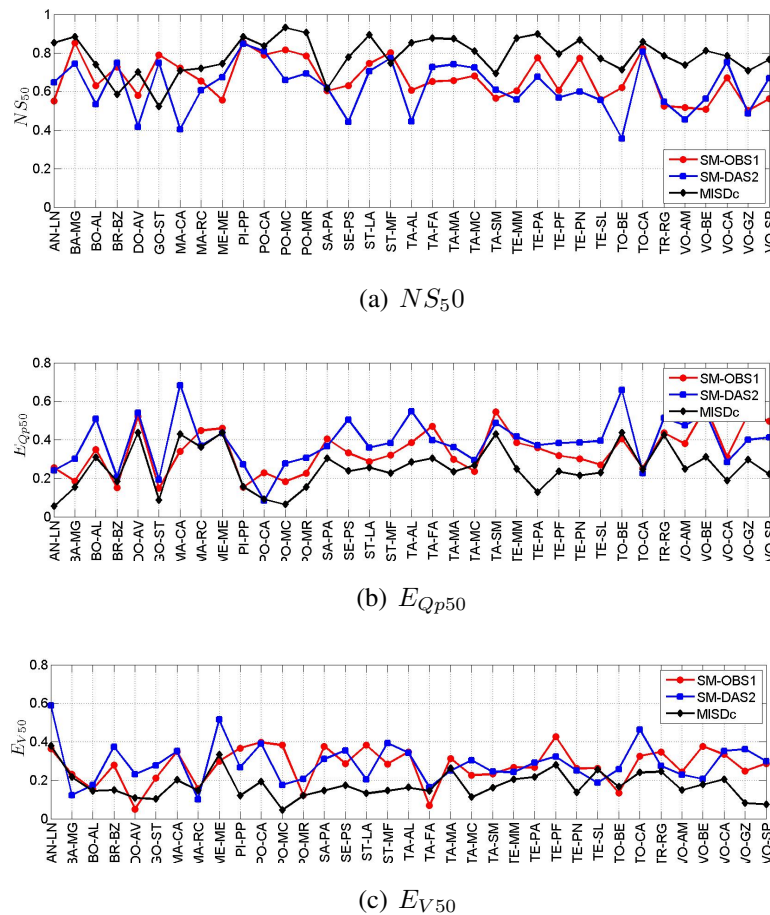

(a) NS_50

(b) E_{Qp50}

(c) E_{V50}

Figure 4. Median performance indexes for the selected catchments, NS_{50} =median Nash–Sutcliffe (**a**); E_{Qp50} = median relative error in peak discharge (**b**); E_{V50} = median relative error in volume (**c**).

The performance of SCRRM with respect to MISDc can be better visualized by the scatter plots shown in Figure 5(a) and 5(b). The figures plot the performance indexes NS_{50}, E_{Qp50} and E_{V50} of MISDc against those of SM-OBS-1 and SM-DAS-2, respectively. Overall, MISDc outperforms SCRRM, but it can be recognized that when MISDc provides a good performance, also SCRRM works well; thus, we may conclude that the results are somehow dependent on the quality of the input data and on the model structure.

Overall, the median of NS, calculated on all selected events, yields 0.65, 0.60 and 0.74, for SM-OBS-1, SM-DAS-2 and MISDc, respectively, while 0.35, 0.40 and 0.25 are obtained for E_{Qp}.

Similarly, E_V provides 0.29, 0.30 and 0.16. Note that MISDc generally outperforms SCRRM in both cases of SM-OBS-1 and SM-DAS-2, except for some catchments (e.g., for NS catchments MA-CA (Magra at Calamazza), GO-ST (Gorzone at Stanghella), ST-MF (Stura di Demonte at Fossano) and BR-BZ; see 4(a); for E_V, also MA-RC (Maira at Raconigi), TA-FA (Tanaro at Farigliano) and TO-BE (Topino at Bettona); see Figure 4(c)). Since the structures of MISDc and SCRRM are very similar (*i.e.*, they rely on the same runoff production and routing models), the only reason for explaining the higher performance is the better estimation of SM at the beginning of the flood event. Indeed, in this study, MISDc is run in lumped mode, providing an estimate of SM for the entire catchment. On the contrary, the SM time series used in SCRRM rely on SM observations from different parts of the basin area; thus, it is likely that the spatial variability of SM is better taken into account by SCRRM. Moreover, SM estimates by MISDc rely on rainfall and temperature measurements, which, other than possibly being affected by many error sources [41], are averaged throughout the basin area, producing possible additional uncertainties [13].
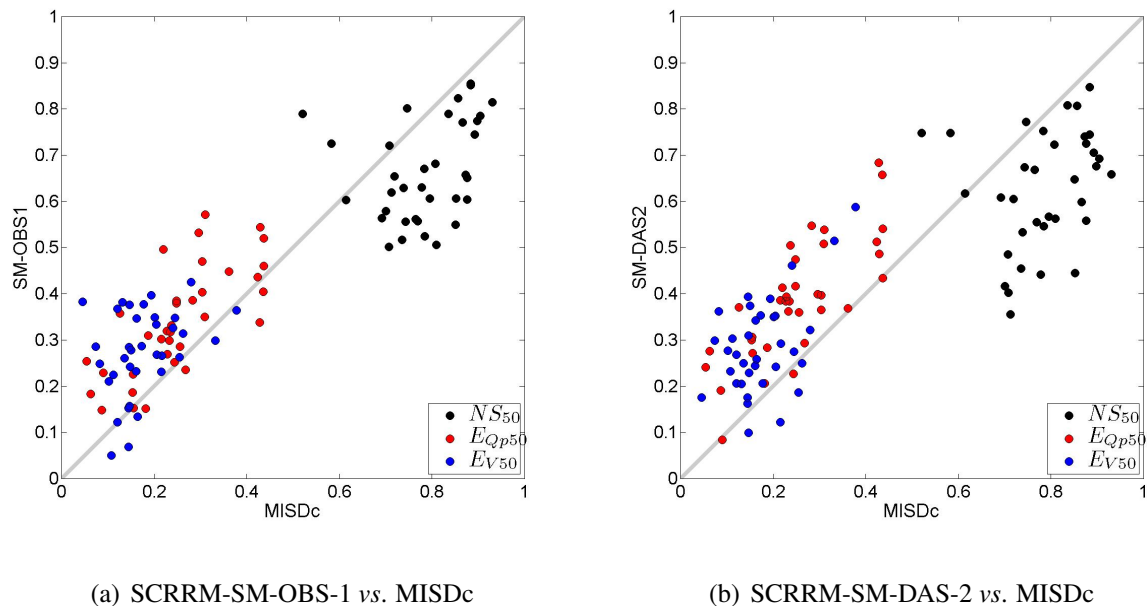

(a) SCRRM-SM-OBS-1 *vs*. MISDc (b) SCRRM-SM-DAS-2 *vs*. MISDc

Figure 5. Comparison between MISDc (Modello Idrologico Semi-Distribuito in continuo) and SCRRM run with SM-OBS-1 (**a**) and SM-DAS-2 (**b**) in terms of median Nash–Sutcliffe, NS_{50}, median relative error on peak discharge, E_{Qp50}, and median relative error in total runoff volume, E_{V50}, for the selected catchments.

To assess if SCRRM results could be affected by catchment area extension, climatic conditions, average temperature and latitude, we calculated $\overline{NS}$ against these variables (not shown for the sake of brevity), but we did not find any strong evidence of any existing trend, except a slight increment of the performances as the area of the catchment is increased. Although we cannot draw any conclusions, because of the relatively small number of catchments analyzed (and the possible errors contained in the observed discharge), this increment is highly expected due to the coarse resolution of SM-OBS-1 and SM-DAS-2. Future investigations will consider a longer dataset and stronger climatic differences for the catchments in order to gain additional information on the SCRRM performances.

Finally, in Figures 6(a) and 7(a), we plotted the simulated and the observed discharge for two representative catchments (TE-SL (Tevere at Santa Lucia) and PO-CA (Po at Carignano)). The respective SM time series in terms of SWI, $\theta_{SM-DAS-2}$ and SM simulated by MISDc are plotted in Figures 6(b) and 7(b). Table 3 summarizes the results obtained for the two catchments.
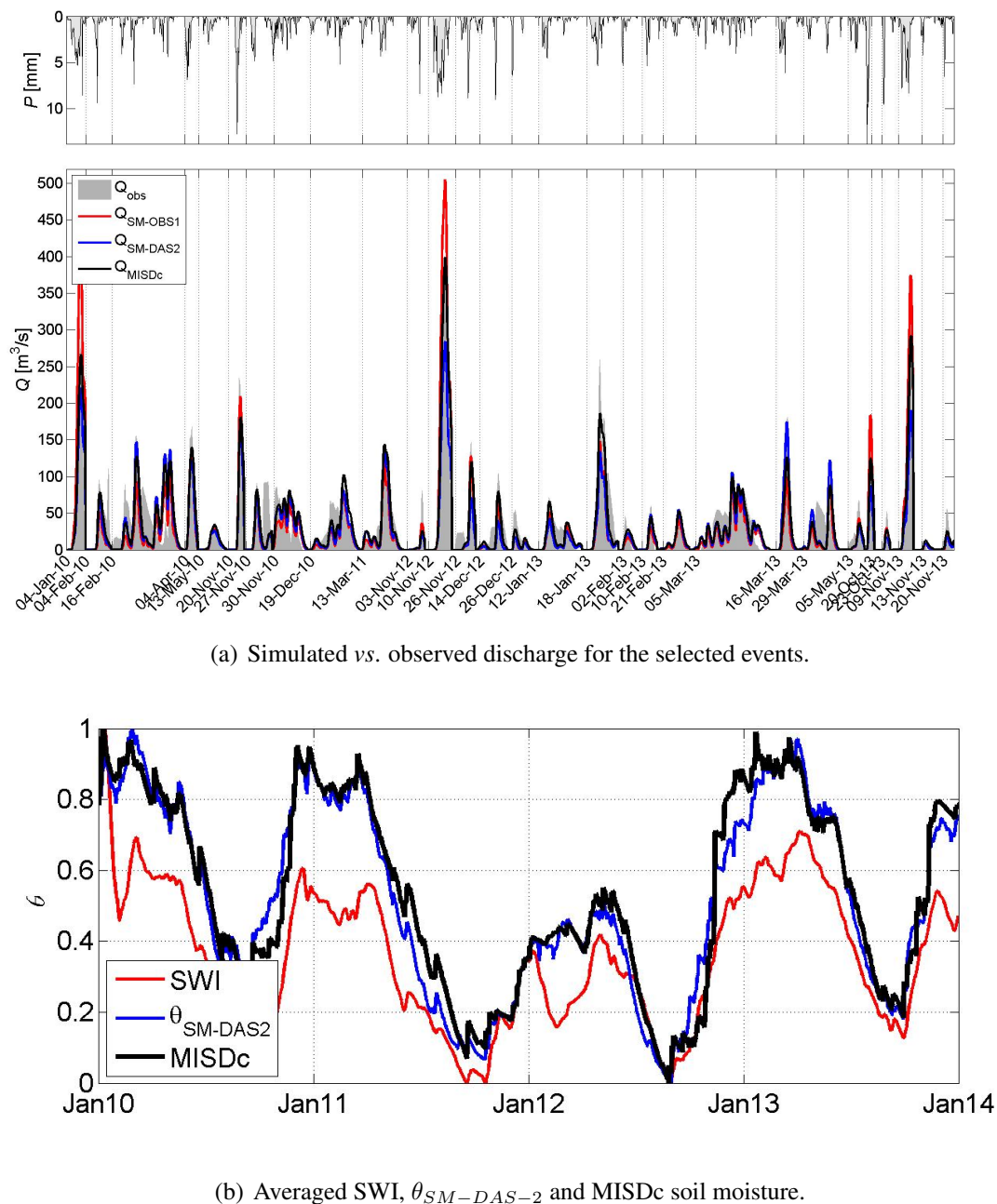

(a) Simulated *vs.* observed discharge for the selected events.

(b) Averaged SWI, $\theta_{SM-DAS-2}$ and MISDc soil moisture.

Figure 6. Observed rainfall (P) and simulated *versus* observed discharge (Q) for the selected events (**a**). Averaged SWI (Soil Water Index)(Equation (1)), $\theta_{SM-DAS-2}$ (Equation (3)) and MISDc soil moisture, θ, from 2010 to 2013 (**b**). Catchment: Tevere River at Santa Lucia (TE-SL).

For TE-SL (with an area of about 840 km^2), the models behave very similar, with MISDc slightly superior to SCRRM for all of the considered performance scores. In particular, SM-OBS-1 tends to

overestimate the direct runoff volume and the peak discharges, both in the mean and in the median, especially for the largest events (see Figure 6(a)), providing the largest values of both E_{Qp} and E_V (see 3). The SM time series show very similar patterns for MISDc and $\theta_{SM-DAS-2}$ ($z = 166$ cm), while SWI seems characterized by a lower variability ($T = 48$ days).
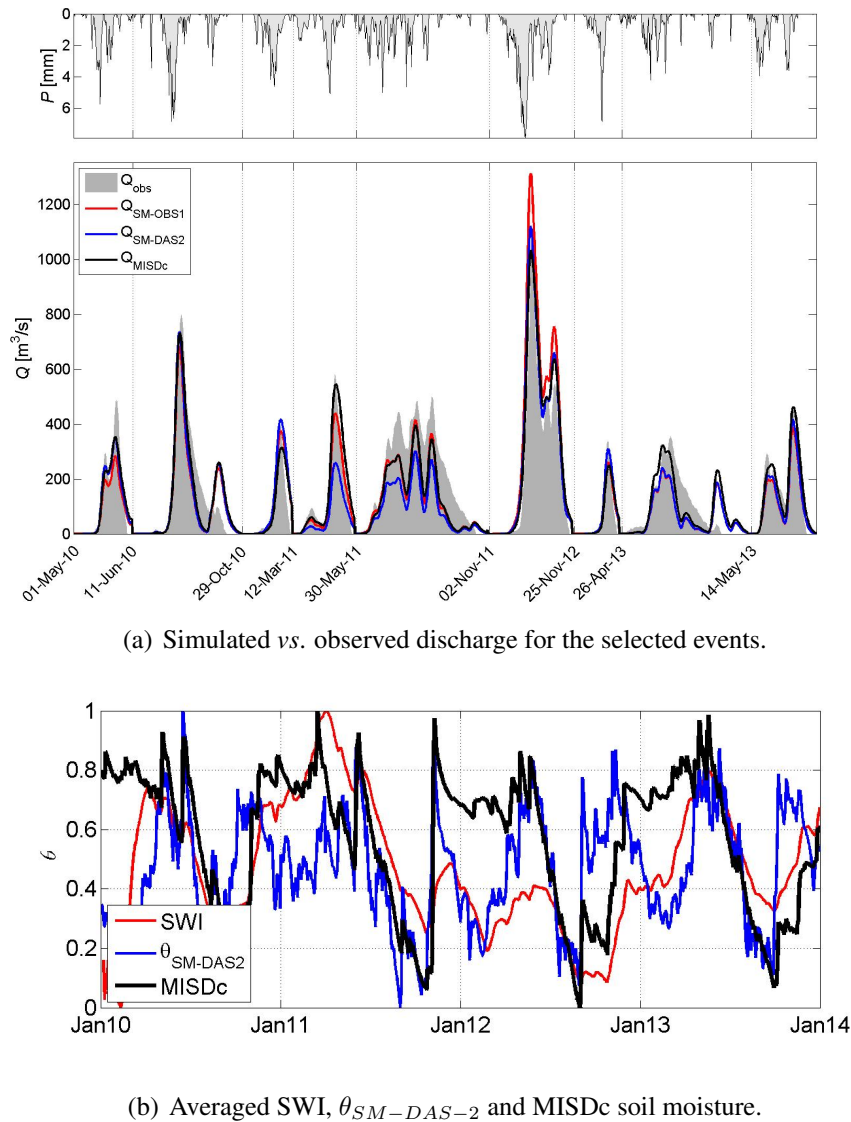

(a) Simulated *vs*. observed discharge for the selected events.

(b) Averaged SWI, $\theta_{SM-DAS-2}$ and MISDc soil moisture.

Figure 7. Observed rainfall (P) and simulated *versus* observed discharge (Q) (**a**). Averaged SWI (Equation (1)), $\theta_{SM-DAS-2}$ (Equation (3)) and MISDc soil moisture, θ, from 2010 to 2013 (**b**). Catchment: Po River at Carignano (PO-CA).

For PO-CA (with an area of about 3570 km^2, four-times the size of TE-SL), all of the models provide good results, both in the mean and in the median scores. A general agreement between the models can be also seen in Figure 6(a). It is interesting to note the good performance obtained by SM-DAS-2, which provides the lowest value of the median E_V. In contrast with TE-SL, the SM time series for PO-CA in 7(b) appear very different with respect to MISDc. Indeed, SWI ($T = 82$ days) and $\theta_{SM-DAS-2}$ ($z = 168$ cm) are the results of the average of multiple pixels falling inside the catchment boundaries of PO-CA; thus, the spatial variability and the inherent errors present in the observed time series may significantly

affect the value of the calibrated parameters, as well as the averaged SM temporal pattern throughout the basin.

Table 3. Summary of the results obtained for the catchments Tevere River at Santa Lucia (TE-SL) and Po River at Carignano (PO-CA).

Catchment	Model	Mean			Median		
		NS	E_{Qp}	E_V	NS	E_{Qp}	E_V
TE-SL	SM-OBS-1	0.452	0.298	0.401	0.558	0.269	0.367
	SM-DAS-2	0.427	0.368	0.354	0.555	0.394	0.268
	MISDc	0.556	0.259	0.180	0.770	0.228	0.121
PO-CA	SM-OBS-1	0.744	0.223	0.253	0.790	0.229	0.210
	SM-DAS-2	0.692	0.213	0.305	0.808	0.084	0.277
	MISDc	0.805	0.135	0.146	0.836	0.090	0.102

4. Conclusions

In this paper, a simplified continuous rainfall-runoff model using SM from external sources for initialization has been used for testing the performance of two operational products (SM-OBS-1 and SM-DAS-2) of the "EUMETSAT Satellite Application Facility in Support of Operational Hydrology and Water Management (H-SAF)" and to gain some knowledge regarding under what conditions SCRRM can be used for operational purposes. The model was applied in 35 catchments of the Italian territory covering different sizes and climate conditions. The performances obtained by SCRRM in flood modelling have been compared against those of a classical continuous model (MISDc, [12]) showing satisfactory results (mean NS equal to 0.61, 0.58 for SM-OBS-1 and SM-DAS-2, respectively), but generally lower than MISDc (mean $NS = 0.66$).

In particular, it was found that:

- In 35 Italian catchments (800 to 7400 km^2), satisfactory results can be obtained by the use SM-OBS-1 and SM-DAS-2 within SCRRM providing a median NS calculated on all of the selected events equal to 0.65 and 0.60, respectively. Similarly, the relative errors in median peak discharge and in runoff volume are 0.35 and 0.29 (SM-OBS-1) and 0.40 and 0.30 (SM-DAS-2). This means that the two products: (i) provide very similar performance and may both be satisfactorily used within SCRRM; and (ii) offer similar information content in flood modelling, which can be efficiently exploited in the context of soil moisture data assimilation in continuous models.

- MISDc generally outperforms SCRRM, except in a few cases. Although this aspect needs further investigation, the reason could be due to the fact that MISDc was run in lumped mode, while SCRRM SM was obtained by averaging the value of SM of different pixels falling inside the catchment boundaries, thus taking more into account for the SM spatial variability. In any case, although the performances of SCRRM are generally lower than those of MISDc (but not by far), they highlight two main interesting issues. First, for operational purposes, SCRRM is expected to be a valuable alternative to a continuous model

in poorly gauged areas, since its structure is less sensitive to problems (not rare) of rain-gauge malfunctions and breakage. Second, the satisfactory results obtained indicate that H-SAF soil moisture products have the potential to improve flood modelling if used with more complex data assimilation schemes with continuous models (*i.e.*, by assimilating SM-OBS-1 and SM-DAS-2 products into the MISDc model).

- Median T and z values, (*i.e.*, the parameters representing the influence of the soil depth in the RR transformation) are 48 days and 100 cm, respectively, which are quite reasonable values in Italy.
- SCRRM can be used as a "hydro-validation tool" to assess the performance of different soil moisture products in terms of the ability to reproduce flood hydrographs. This is a new method for validating soil moisture data that has not been used before.

Overall, we can conclude that both products, SM-OBS-1 and SM-DAS-2, contain sufficient information for satisfactorily reproducing floods. The SCRRM benefits are the possibility to be used in poorly gauged areas (e.g., in areas characterized by discontinuous measures of rainfall and temperature), its simplicity and parsimony, which facilitate setup and operational use. On the other hand, it must be said that in areas characterized by dense and robust hydro-meteorological networks, like the ones used in this paper, a continuous modelling approach is preferable, since it allows one to obtain better performance. In this context, the satellite soil moisture products could be optimally integrated into the continuous model for obtaining a better modelling chain for flood forecasting. Future applications of the model will consider the use of satellite rainfall observations in order to rely completely on satellite data.

Acknowledgments

Author Contributions

All authors contributed extensively to the work presented in this paper. Specific contributions included the development of the SCRRM and MISDc models (Christian Massari, Luca Brocca), of the two H-SAF soil moisture products SM-OBS-1 (Wolfgang Wagner) and SM-DAS-2 (Clement Albergel, Patricia de Rosnay), acquisition and processing of ground-based hydrometeorological data (Simone Gabellani, Silvia Puca, Luca Ciabatta), and preparation of the manuscript and figures (Christian Massari, Luca Brocca, Luca Ciabatta, Tommaso Moramarco). All co-authors contributed to the editing of the manuscript and to the discussion and interpretation of the results.

Conflicts of Interest

The authors declare no conflict of interest.

References

1. Jongman, B.; Hochrainer-Stigler, S.; Feyen, L.; Aerts, J.C.J.H.; Mechler, R.; Botzen, W.J.W.; Bouwer, L.M.; Pflug, G.; Rojas, R.; Ward, P.J. Increasing stress on disaster-risk finance due to large floods. *Nat. Clim. Chang.* **2014**, *4*, 264–268.

2. Brocca, L.; Melone, F.; Moramarco, T. On the estimation of antecedent wetness conditions in rainfall-runoff modelling. *Hydrol. Process.* **2008**, *642*, 629–642.

3. Coustau, M.; Bouvier, C.; Borrell-Estupina, V.; Jourde, H. Flood modelling with a distributed event-based parsimonious rainfall-runoff model: Case of the karstic Lez river catchment. *Nat. Hazard. Earth Syst. Sci.* **2012**, *12*, 1119–1133.

4. Beck, H.E.; Jeu, R.A.M.D.; Schellekens, J.; Dijk, A.I.J.M.V.; Bruijnzeel, L.A. Improving curve number based storm runoff estimates using soil moisture proxies. *IEEE J. Sel. Top. Appl. Earth Obs. Remote Sens.* **2010**, *2*, 250–259.

5. Tramblay, Y.; Bouaicha, R.; Brocca, L.; Dorigo, W.; Bouvier, C.; Camici, S.; Servat, E. Estimation of antecedent wetness conditions for flood modelling in northern Morocco. *Hydrol. Earth Syst. Sci.* **2012**, *16*, 4375–4386.

6. Viviroli, D.; Mittelbach, H.; Gurtz, J.; Weingartner, R. Continuous simulation for flood estimation in ungauged mesoscale catchments of Switzerland–Part II: Parameter regionalisation and flood estimation results. *J. Hydrol.* **2009**, *377*, 208–225.

7. Van Steenbergen, N.; Willems, P. Increasing river flood preparedness by real-time warning based on wetness state conditions. *J. Hydrol.* **2013**, *489*, 227–237.

8. Aronica, G.; Candela, A. A regional methodology for deriving flood frequency curves (FFC) in partially gauged catchments with uncertain knowledge of soil moisture conditions. In Proceedings of iEMSs, Osnabru, Germany, 14–17 June 2004; pp. 1147–1183.

9. Brocca, L.; Melone, F.; Moramarco, T.; Morbidelli, R. Antecedent wetness conditions based on ERS scatterometer data. *J. Hydrol.* **2009**, *364*, 73–87.

10. Brocca, L.; Melone, F.; Moramarco, T.; Singh, V.P. Assimilation of observed soil moisture data in storm rainfall-runoff modeling. *J. Hydrol. Eng.* **2009**, *14*, 153–165.

11. Tramblay, Y.; Bouvier, C.; Martin, C.; Didon-Lescot, J.F.; Todorovik, D.; Domergue, J.M. Assessment of initial soil moisture conditions for event-based rainfall-runoff modelling. *J. Hydrol.* **2010**, *387*, 176–187.

12. Brocca, L.; Melone, F.; Moramarco, T. Distributed rainfall-runoff modelling for flood frequency estimation and flood forecasting. *Hydrol. Process.* **2011**, *25*, 2801–2813.

13. Tramblay, Y.; Bouvier, C.; Ayral, P.A.; Marchandise, A. Impact of rainfall spatial distribution on rainfall-runoff modelling efficiency and initial soil moisture conditions estimation. *Nat. Hazard. Earth Syst. Sci.* **2011**, *11*, 157–170.

14. Aubert, D.; Loumagne, C.; Oudin, L. Sequential assimilation of soil moisture and streamflow data in a conceptual rainfall-runoff model. *J. Hydrol.* **2003**, *280*, 145–161.

15. Dorigo, W.A.; Wagner, W.; Hohensinn, R.; Hahn, S.; Paulik, C.; Xaver, A.; Gruber, A.; Drusch, M.; Mecklenburg, S.; van Oevelen, P.; *et al.* The International Soil Moisture Network: A data hosting facility for global in situ soil moisture measurements. *Hydrol. Earth Syst. Sci.* **2011**, *15*, 1675–1698.

16. Bartalis, Z.; Wagner, W.; Naeimi, V.; Hasenauer, S.; Scipal, K.; Bonekamp, H.; Figa, J.; Anderson, C. Initial soil moisture retrievals from the METOP-A Advanced Scatterometer (ASCAT). *Geophys. Res. Lett.* **2007**, *34*, L20401.

17. Owe, M.; de Jeu, R.; Holmes, T. Multisensor historical climatology of satellite-derived global land surface moisture. *J. Geophys. Res.* **2008**, *113*, F01002.

18. Kerr, Y.H.; Waldteufel, P.; Wigneron, J.P.; Delwart, S.; Cabot, F.; Boutin, J.; Escorihuela, M.J.; Font, J.; Reul, N.; Gruhier, C.; *et al.* The SMOS mission: New tool for monitoring key elements of the global water cycle. *Proc. IEEE* **2010**, *98*, 666–687.

19. Balsamo, G.; Albergel, C.; Beljaars, A.; Boussetta, S.; Brun, E.; Cloke, H.; Dee, D.; Dutra, E.; Pappenberger, F.; de Rosnay, P.; *et al.* ERA-Interim/Land: A global land-surface reanalysis based on ERA-Interim meteorological forcing. *Era Rep. Series* **2012**, *13*, 1–25.

20. Wagner, W.; Bloschl, G.; Pampaloni, P.; Calvet, J.; Bizzarri, B.; Wigneron, J.; Kerr, Y. Operational readiness of microwave remote sensing of soil moisture for hydrologic applications. *Nordic Hydrol.* **2007**, *38*, 1–20.

21. Liu, Y.; Weerts, A.H.; Clark, M.; Hendricks Franssen, H.J.; Kumar, S.; Moradkhani, H.; Seo, D.J.; Schwanenberg, D.; Smith, P.; van Dijk, A.I.J.M.; *et al.* Advancing data assimilation in operational hydrologic forecasting: Progresses, challenges, and emerging opportunities. *Hydrol. Earth Syst. Sci.* **2012**, *16*, 3863–3887.

22. Reichle, R.H. Bias reduction in short records of satellite soil moisture. *Geophys. Res. Lett.* **2004**, *31*, L19501.

23. Crow, W.T.; Van Loon, E. Impact of incorrect model error assumptions on the sequential assimilation of remotely sensed surface soil moisture. *J. Hydrometeorol.* **2006**, *7*, 421–432.

24. Massari, C.; Brocca, L.; Barbetta, S.; Papathanasiou, C.; Mimikou, M.; Moramarco, T. Using globally available soil moisture indicators for flood modelling in Mediterranean catchments. *Hydrol. Earth Syst. Sci.* **2014**, *18*, 839–853.

25. Todini, E. Rainfall-runoff modeling—Past, present and future. *J. Hydrol.* **1988**, *100*, 341–352.

26. Beven, K.; Freer, J. A dynamic TOPMODEL. *Hydrol. Process.* **2001**, *15*, 1993–2011.

27. Famiglietti, J.S.; Wood, E.F. Multiscale modeling of spatially variable water and energy balance processes. *Water Resour. Res.* **1994**, *30*, 3061–3078.

28. Pignone, F.; Rebora, N.; Silvestro, F.; Castelli, F. *GRISO (Generatore Random di Interpolazioni Spaziali da Osservazioni incerte). Relazione delle attività del I anno inerente la Convenzione 778/2009 tra Dipartimento di Protezione Civile e Fondazione CIMA (Centro Internazionale in Monitoraggio Ambientale)*; Technical Report No. 272, Savona, Italy, pp. 353, 2010.

29. Melone, F.; Corradini, C.; Singh, V.P. Lag prediction in ungauged basins: An investigation through actual data of the upper Tiber River valley. *Hydrol. Process.* **2002**, *16*, 1085–1094.

30. Wagner, W.; Lemoine, G.; Rott, H. A method for estimating soil moisture from ERS scatterometer and soil data. *Remote Sens. Environ.* **1999**, *70*, 191–207.

31. Brocca, L.; Melone, F.; Moramarco, T.; Wagner, W.; Naeimi, V.; Bartalis, Z.; Hasenauer, S. Improving runoff prediction through the assimilation of the ASCAT soil moisture product. *Hydrol. Earth Syst. Sci.* **2010**, *14*, 1881–1893.

32. Albergel, C.; Rüdiger, C.; Carrer, D.; Calvet, J.C.; Fritz, N.; Naeimi, V.; Bartalis, Z.; Hasenauer, S. An evaluation of ASCAT surface soil moisture products with *in-situ* observations in Southwestern France. *Hydrol. Earth Syst. Sci.* **2009**, *13*, 115–124.

33. De Rosnay, P.; Drusch, M.; Vasiljevic, D.; Balsamo, G.; Albergel, C.; Isaksen, L. A simplified Extended Kalman Filter for the global operational soil moisture analysis at ECMWF. *Q. J. R. Meteorol. Soc.* **2013**, *139*, 1199–1213.

34. Albergel, C.; de Rosnay, P.; Gruhier, C.; Muñoz Sabater, J.; Hasenauer, S.; Isaksen, L.; Kerr, Y.; Wagner, W. Evaluation of remotely sensed and modelled soil moisture products using global ground-based *in situ* observations. *Remote Sens. Environ.* **2012**, *118*, 215–226.

35. Melone, F.; Neri, N.; Morbidelli, R.; Saltalippi, C. A conceptual model for flood prediction in basins of moderate size. In *Applied simulation and Modeling*; Hamza, M.H., Ed.; IASTED Acta Press: Anaheim, CA, USA, 2001; pp. 461–466.

36. Kim, N.; Lee, J. Temporally weighted average curve number method for daily runoff simulation. *Hydrol. Process.* **2008**, *4948*, 4936–4948.

37. Gupta, V.; Waymire, C. A representation of an instantaneous unit hydrograph from geomorphology. *Water Resour. Res.* **1980**, *16*, 855–862.

38. Moramarco, T.; Melone, F.; Singh, V.P. Assessment of flooding in urbanized ungauged basins: A case study in the Upper Tiber area, Italy. *Hydrol. Process.* **2005**, *19*, 1909–1924.

39. Nash, J.; Sutcliffe, J. River flow forecasting through conceptual models part I—A discussion of principles. *J. Hydrol.* **1970**, *10*, 282–290.

40. Bober, W. *Introduction to Numerical and Analytical Methods with MATLAB for Engineers and Scientists*; CRC Press, Inc.: Boca Raton, FL, USA, 2013.

41. Crow, W.T.; van den Berg, M.J.; Huffman, G.J.; Pellarin, T. Correcting rainfall using satellite-based surface soil moisture retrievals: The Soil Moisture Analysis Rainfall Tool (SMART). *Water Resour. Res.* **2011**, *47*, W08521.